



Synthesis, characterisation and crystal structures of Schiff bases from the reaction of 4,6-*O*-ethylidene- β -D-glucopyranosylamine with substituted salicylaldehydes

Ajay K. Sah,^a Chebrolu P. Rao,^{a,*} Pauli K. Saarenketo,^b Erkki Kolehmainen,^b Kari Rissanen^b

^a*Bioinorganic Laboratory, Department of Chemistry, Indian Institute of Technology Bombay, Powai, Mumbai 400 076, India*

^b*Department of Chemistry, University of Jyväskylä, Jyväskylä Fin 40351, Finland*

Received 26 May 2001; accepted 9 July 2001

Abstract

Multiple chemical modifications were carried out on D-glucose to result in the corresponding Schiff bases. Such modifications performed on D-glucose not only helped in increasing the solubility of the products in nonaqueous solvents, but also restricted the anomerisation of the saccharide moiety in solution. NMR study of the products revealed the presence of the β -anomeric form of the saccharide moiety in Me₂SO solution. All the compounds were characterised by analytical and spectral methods. The literature is devoid of any crystal structures of saccharide–Schiff base combinations of the type reported in this paper. The crystal structures of these molecules exhibited a tridentate, ONO binding core. These studies further revealed that the compounds in the solid state were in the β -D-pyranose form with the ⁴C₁ chair conformation. The compounds exhibited interesting lattice structures assisted through weak interactions of the type O–H \cdots O and C–H \cdots O. The lattice structure of one of these compounds exhibited channels filled with chloroform molecules. © 2001 Elsevier Science Ltd. All rights reserved.

Keywords: 4,6-*O*-Ethylidene- β -D-glucopyranosylamine; Saccharide–Schiff bases; Single crystal XRD; Channel structure; Tridentate binding core; FAB mass spectrometry

1. Introduction

It is well known that under mild conditions, aldoses react with primary or secondary amines to form glycosylamines where the hydroxyl group on C-1 is replaced by the amine in order to result in C-1–NRR' via condensation. The glycosylamines are of biological and pharmaceutical importance.¹ Many of these

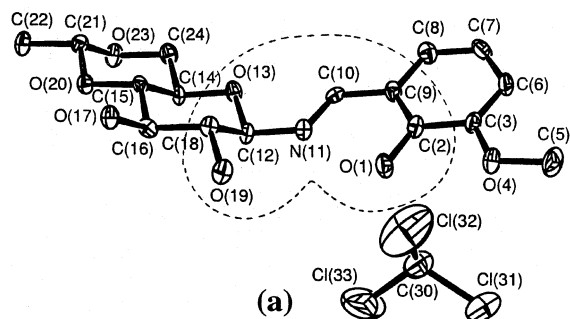
are considered as active-site-directed reversible inhibitors of glycosidase, and some of these compounds have been proposed as oral anti-diabetic agents.^{2–4} Several glycosylamines are known in the literature, but as far as the glycosylamine derived Schiff base molecules are concerned, the literature is scarce. Although Schiff base molecules are potential ligands for the metal–ion binding, it is surprising to note that the inorganic chemists have not much explored the potential of the saccharide-based Schiff bases. This may be attributed to the problem of the rearrange-

* Corresponding author. Tel.: +91-22-5783245; fax: +91-22-5723480.

E-mail address: cprao@chem.iitb.ac.in (C.P. Rao).

Table 1
Summary of crystallographic data and structural parameters for **1** and **2**

	1	2
Empirical formula	C ₁₇ H ₂₂ Cl ₃ NO ₇	C ₁₅ H ₁₈ BrNO ₆
Molecular weight	458.71	388.21
<i>T</i> (K)	173(2)	173(2)
Crystal system	monoclinic	monoclinic
Space group	<i>P</i> 2 ₁	<i>P</i> 2 ₁
Cell constants		
<i>a</i> (Å)	11.898(1)	8.439(1)
<i>b</i> (Å)	6.295(1)	5.601(1)
<i>c</i> (Å)	14.718(1)	16.456(1)
β (°)	101.06(1)	92.01(1)
<i>V</i> (Å ³)	1081.9(2)	777.34(17)
<i>Z</i>	2	2
<i>D</i> _{calcd} (Mg m ⁻³)	1.408	1.659
Total Reflections	6384	4544
Unique reflections	3543	3011
	[<i>R</i> _{int} = 0.0424]	[<i>R</i> _{int} = 0.0340]
Max/min transmission factors	0.9008 and 0.8514	0.5937 and 0.5586
Parameters	262	217
Final <i>R</i> (<i>I</i> > 2σ(<i>I</i>))	0.0657	0.0290
<i>R</i> _w	0.1521	0.0623



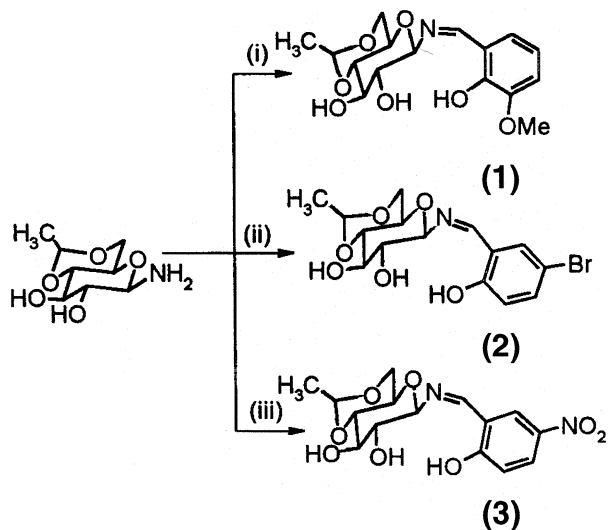
(b)

Fig. 1. (a) Molecular structure of **1** and (b) its stereoview showing 50% probability thermal ellipsoids using ORTEP. The dashed line enclosure shown in (a) represents the ONO binding core.

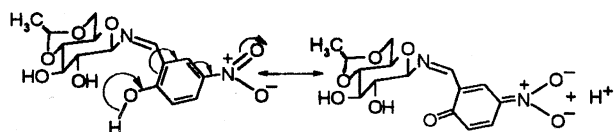
Table 2

Atomic coordinates ($\times 10^4$) for **1**

	<i>x</i>	<i>y</i>	<i>z</i>
C(2)	7524(4)	7801(8)	4124(3)
C(3)	7926(4)	5969(8)	4649(3)
C(5)	9213(5)	3027(9)	4809(4)
C(6)	7542(4)	5511(8)	5449(4)
C(7)	6730(5)	6843(8)	5743(4)
C(8)	6322(4)	8604(8)	5249(3)
C(9)	6718(4)	9117(7)	4427(3)
C(10)	6290(4)	11027(8)	3899(3)
C(12)	6223(4)	13324(7)	2619(3)
C(14)	4925(4)	16211(7)	2478(3)
C(15)	4362(4)	15539(7)	1503(3)
C(16)	5228(4)	14504(8)	1030(3)
C(18)	5728(4)	12600(7)	1623(3)
C(21)	3028(4)	18323(8)	1450(3)
C(22)	2497(4)	20168(8)	880(3)
C(24)	4038(4)	17315(8)	2922(3)
N(11)	6639(3)	11498(6)	3158(3)
O(1)	7928(3)	8175(5)	3344(2)
O(4)	8704(3)	4814(6)	4283(2)
O(13)	5341(3)	14374(5)	3002(2)
O(17)	4685(3)	13868(5)	127(2)
O(19)	6627(3)	11645(6)	1260(2)
O(20)	3859(3)	17356(5)	994(2)
O(23)	3552(3)	19042(5)	2339(2)
C(30)	9826(5)	5934(10)	2508(4)
Cl(31)	11099(1)	4685(3)	3058(1)
Cl(32)	8995(2)	4160(6)	1750(2)
Cl(33)	10135(3)	8326(5)	2065(4)



Scheme 1. Glycosylamine-based Schiff base compounds. (i) 3-Methoxysalicylaldehyde; (ii) 5-bromosalicylaldehyde; (iii) 5-nitrosalicylaldehyde.



Scheme 2. Resonance stabilisation in Schiff base **3**.

ment of the glycosylamines in solution via the formation of imonium ion intermediates, resulting in mutarotation, hydrolysis, transglycosylation, or Amadori rearrangements.⁵ To our knowledge, the structurally characterised complex of C-1 amine based Schiff base ligand is the tetranuclear copper complex reported for 1-amino-1-deoxy-D-sorbitol based Schiff base ligand in the literature.⁶ Therefore, herein we report the synthesis and characterisation of the Schiff base molecules derived from 4,6-*O*-

ethylidene- β -D-glucopyranosylamine. All the products were characterised based on FTIR, UV–Vis, NMR, FAB mass spectrometry, microanalysis and single-crystal X-ray diffraction studies.

2. Experimental

D-Glucose was procured from Aldrich Chemical Co. (USA) and 3-methoxysalicyl-

Table 3
Anisotropic displacement parameters ($\text{\AA}^2 \times 10^3$) for **1**

	U^{11}	U^{22}	U^{33}	U^{23}	U^{13}	U^{12}
C(2)	26(3)	19(3)	18(2)	1(2)	−2(2)	2(2)
C(3)	20(2)	17(3)	28(3)	3(2)	−3(2)	3(2)
C(5)	38(3)	21(3)	57(4)	7(3)	−1(3)	10(2)
C(6)	27(3)	22(3)	34(3)	16(2)	−3(2)	−1(2)
C(7)	33(3)	30(3)	24(3)	10(2)	3(2)	−12(2)
C(8)	28(3)	24(3)	22(3)	1(2)	4(2)	−1(2)
C(9)	25(2)	13(3)	19(2)	2(2)	−3(2)	−2(2)
C(10)	12(2)	20(3)	25(3)	−2(2)	5(2)	1(2)
C(12)	20(2)	19(3)	18(2)	1(2)	0(2)	5(2)
C(14)	20(2)	17(2)	14(2)	5(2)	0(2)	4(2)
C(15)	21(2)	11(2)	19(2)	4(2)	4(2)	2(2)
C(16)	24(2)	18(3)	16(2)	−4(2)	5(2)	−6(2)
C(18)	22(3)	17(2)	20(2)	−2(2)	4(2)	2(2)
C(21)	19(2)	19(3)	21(2)	0(2)	5(2)	0(2)
C(22)	30(3)	24(3)	24(3)	6(2)	−1(2)	11(2)
C(24)	31(3)	21(3)	20(3)	1(2)	6(2)	4(2)
N(11)	24(2)	19(2)	18(2)	1(2)	0(2)	3(2)
O(1)	34(2)	24(2)	25(2)	8(2)	10(2)	10(2)
O(4)	32(2)	23(2)	37(2)	9(2)	4(2)	10(2)
O(13)	30(2)	16(2)	17(2)	0(1)	6(1)	5(1)
O(17)	29(2)	23(2)	14(2)	−3(1)	2(1)	3(1)
O(19)	31(2)	26(2)	21(2)	−4(2)	4(2)	9(2)
O(20)	24(2)	17(2)	19(2)	1(1)	4(1)	3(1)
O(23)	31(2)	18(2)	22(2)	−3(1)	0(1)	7(2)
C(30)	36(3)	55(4)	54(4)	4(3)	8(3)	7(3)
Cl(31)	34(1)	81(1)	78(1)	5(1)	7(1)	10(1)
Cl(32)	92(2)	165(3)	89(2)	−55(2)	−24(1)	12(2)
Cl(33)	101(2)	116(2)	322(5)	138(3)	119(3)	48(2)

The anisotropic displacement factor exponent takes the form: $-2\pi^2[h^2a^{*2}U^{11} + \dots + 2hka \times b \times U^{12}]$.

Table 4
Selected torsion angles ($^\circ$) for **1**

N(11)–C(12)–O(13)–C(14)	179.4(4)	N(11)–C(12)–C(18)–C(16)	177.7(4)
O(13)–C(12)–C(18)–O(19)	178.0(4)	C(15)–C(16)–C(18)–O(19)	−175.0(4)
O(17)–C(16)–C(18)–C(12)	−175.5(3)	C(14)–C(15)–C(16)–O(17)	179.4(4)
O(20)–C(15)–C(16)–C(18)	179.5(3)	O(13)–C(14)–C(15)–O(20)	175.4(3)
C(24)–C(14)–C(15)–C(16)	178.1(4)	C(24)–C(14)–O(13)–C(12)	−177.8(4)
C(9)–C(10)–N(11)–C(12)	178.8(4)	C(2)–C(9)–C(10)–N(11)	0.5(6)

Table 5
Cremer–Pople puckering parameters and asymmetry parameters

	1	2
Q (Å)	0.603	0.595
θ (°)	2.2	8.9
ϕ (°)	278.07	286.36
ΔC_s (C-1, C-4) (°)	0	0
ΔC_s (C-2, C-5) (°)	0	0
ΔC_s (C-3, O-5) (°)	0	0

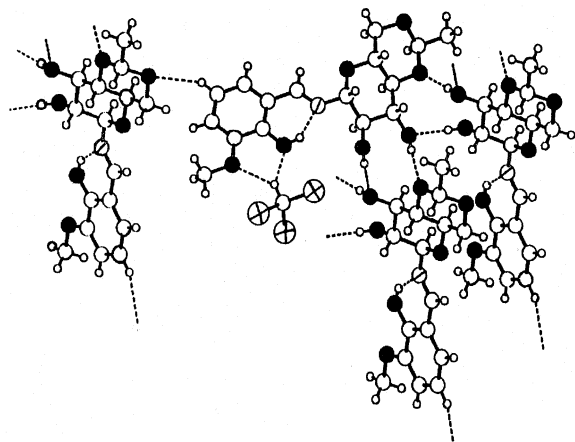


Fig. 2. H-bonding pattern observed in **1**. The filled circles denote oxygen atoms, circles bisected with one line denote nitrogen atoms and circles with cross denote chlorine atoms. Dotted lines represent H-bonds.

aldehyde from Lancaster Synthesis Ltd (UK). 4,6-*O*-Ethylidene- β -D-glucopyranose,⁷ 4,6-*O*-ethylidene- β -D-glucopyranosylamine⁸ (EGNH₂) and 5-bromosalicylaldehyde were synthesised as per the reported procedures,⁹ and all other chemicals were procured from local sources. All the solvents were purified and dried immediately before use. Elemental analysis was carried out on a Carlo–Erba elemental analyser, and FTIR spectra were recorded on a Nicolet Impact 400 instrument in KBr matrix. Absorption spectra were measured on a Shimadzu UV2101PC spectrophotometer. ¹H NMR spectra were recorded on Bruker Avance DRX 500 or Varian XL-300 spectrometer in Me₂SO-*d*₆. The FAB mass spectra were recorded on a JEOL SX 102/DA-600 mass spectrometer/data system using argon/xenon (6 kV, 10 mA) as the FAB gas and *m*-nitrobenzyl alcohol as the matrix. The accelerating voltage was 10 kV, and the spectra

were recorded at room temperature. Short labels, such as, ‘Sac’, ‘Prot’ and ‘Ar’ are used in the NMR spectral assignments in order to refer to the saccharide, protection and aromatic groups, respectively.

N-(2-Hydroxy-3-methoxybenzylidene)-4,6-*O*-ethylidene- β -D-glucopyranosylamine (**1**).—To a suspension of 4,6-*O*-ethylidene- β -D-glucopyranosylamine (EGNH₂, 5.12 g, 24.97 mmol) in EtOH (40 mL), 3-methoxysalicylaldehyde (3.82 g, 25.11 mmol) was added, and the reaction mixture was allowed to reflux for 2.5 h, which resulted in a clear orange solution. The reaction mixture was allowed to cool to rt, and the solvent was evaporated to result in a pasty mass. This was further dissolved in CH₂Cl₂ (10 mL), and excess petroleum ether was added to precipitate the product. The product was isolated through filtration, and the filtrate was concentrated and kept at –20 °C to result in a second crop of solid. Yield 8.08 g (93%); mp 130–132 °C. UV–Vis [λ_{\max} ; nm (ϵ ; L cm⁻¹ mol⁻¹)]: 267 (21667), 334 (4408), 419 (86). ¹H NMR (Me₂SO-*d*₆, 300 MHz, ppm): 13.01 (1 H, s, ArOH), 8.57 (1 H, s, HC=N), 7.09 (2 H, m, ArH), 6.85 (1 H, t, *J* 7.9 Hz, ArH), 5.54 (1 H, d, *J* 5.9 Hz, SacOH), 5.35 (1 H, d, *J* 5.5 Hz, SacOH), 4.75 (1 H, q, *J* 4.9 Hz, ProtCH), 4.56 (1 H, d, *J* 8.4 Hz, SacH-1), 4.06 (1 H, m, SacH-5), 3.79 (3 H, s, ArCH₃), 3.0–3.6 (5 H, m, Sac), 1.25 (3 H, d, *J* 5.1 Hz, ProtCH₃). ¹³C NMR (Me₂SO-*d*₆, 126 MHz, ppm): 165.4, 150.6, 147.8, 123.7, 118.3, 118.2, 115.4, 98.6, 95.2, 80.1, 74.7, 73.3, 67.9, 67.2, 55.8, 20.3. FABMS: *m/z* 340 (M + H⁺, 100%). Anal. Calcd for C₁₆H₂₂NO_{7.5}: C, 55.16; H, 6.22; N, 4.02. Found C, 55.40; H, 6.56; N, 4.16. Single crystals suitable for X-ray diffraction studies were grown by slow diffusion of CHCl₃ into a concentrated solution of the compound in MeOH at rt.

N-(5-Bromo-2-hydroxybenzylidene)-4,6-*O*-ethylidene- β -D-glucopyranosylamine (**2**).—This compound was prepared by a procedure similar to that adopted for **1**, but by using EGNH₂ (2.77 g, 13.51 mmol) and 5-bromosalicylaldehyde (2.77 g, 13.78 mmol) in MeOH (40 mL). Yield 4.36 g (83%); mp 171–72 °C. UV–Vis [λ_{\max} ; nm (ϵ ; L cm⁻¹ mol⁻¹)]: 261 (15620), 330 (7154), 414 (61). ¹H NMR

(Me₂SO-*d*₆, 300 MHz, ppm): 12.91 (1 H, s, ArOH), 8.57 (1 H, s, HC=N), 7.80 (1 H, d, *J* 2.6 Hz, ArH), 7.50 (1 H, dd, *J* 2.6, 8.8 Hz, ArH), 6.89 (1 H, d, *J* 8.8 Hz, ArH), 5.57 (1 H, d, *J* 5.7 Hz, SacOH), 5.37 (1 H, d, *J* 5.5 Hz, SacOH), 4.75 (1 H, q, *J* 5.0 Hz, ProtCH), 4.58 (1 H, d, *J* 8.2 Hz, SacH-1), 4.06 (1 H, m, SacH-5), 3.0–3.5 (5 H, m, Sac), 1.25 (3 H, d, *J* 4.9 Hz, ProtCH₃). ¹³C NMR (Me₂SO-*d*₆, 126 MHz, ppm): 163.3, 159.3, 135.2, 133.8, 120.3, 118.9, 109.5, 98.5, 95.0, 80.0, 74.6, 73.2, 67.8,

67.2, 20.2. FABMS *m/z* 388 (M⁺, 100%). Anal. Calcd for C₁₅H₁₈BrNO₆: C, 46.41; H, 4.67; N, 3.61. Found C, 46.72; H, 4.76; N, 3.31. Single crystals suitable for X-ray diffraction studies were grown by slow evaporation of a concentrated solution in MeOH at rt.

N-(2-Hydroxy-5-nitrobenzylidene)-4,6-O-ethylidene-β-D-glucopyranosylamine (3).— This compound was prepared by adopting the procedure given for 1 but using EGNH₂ (0.41 g, 2.00 mmol) and 5-nitrosalicylaldehyde (0.34

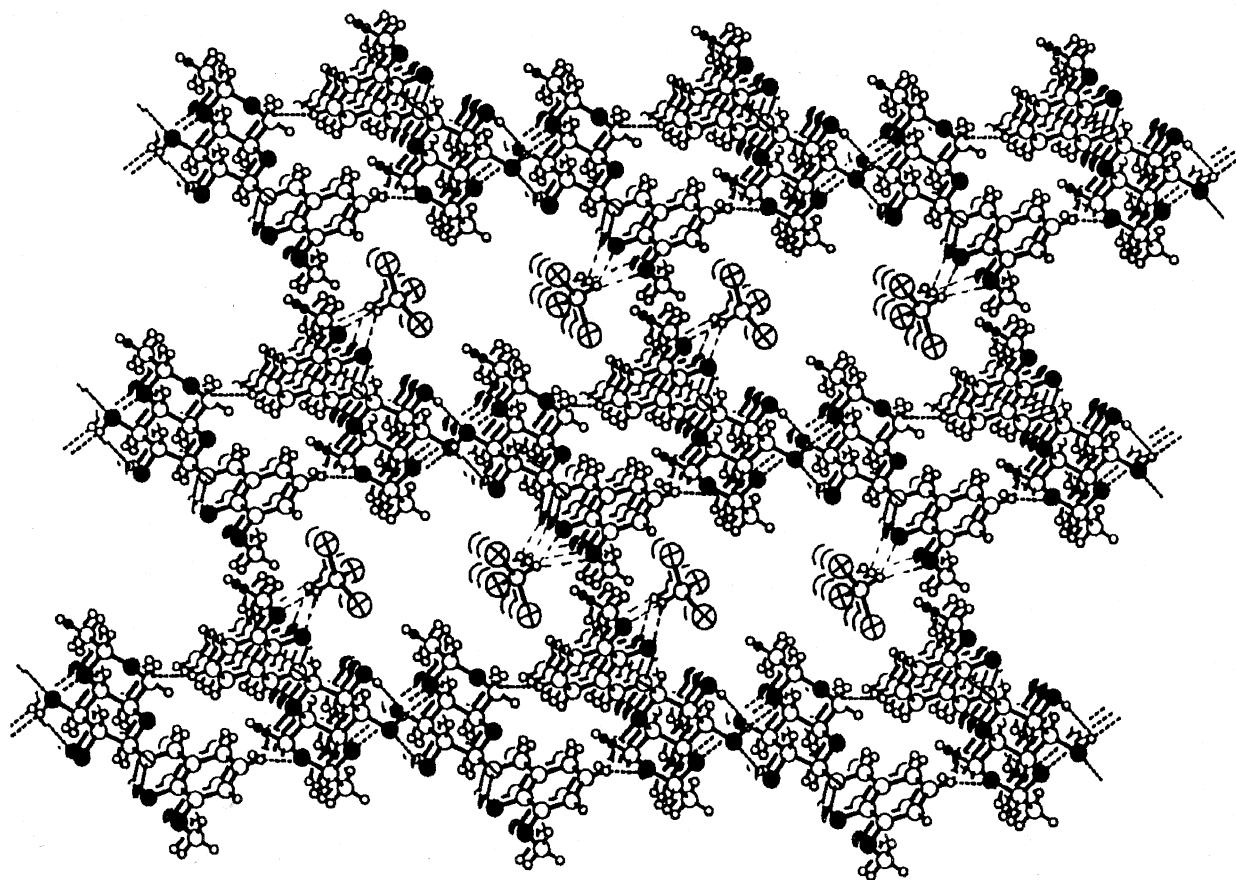


Fig. 3. Packing diagram of 1 showing channels filled with chloroform molecules. The filled circles denote oxygen atoms, circles bisected with one line denote nitrogen atoms and circles with cross denote chlorine atoms. Dotted lines represent H-bonds.

Table 6
Hydrogen bond data in the case of 1

D–H⋯A	d(D–H) (Å)	d(H⋯A) (Å)	d(D⋯A) (Å)	<(DHA) (°)	Symmetry
O(1)–H(1)⋯N(11)	0.838(10)	1.814(3)	2.577(5)	150.5(5)	
O(17)–H(17)⋯O(20)	0.839(10)	1.964(2)	2.779(5)	163.5(6)	1– <i>x</i> , –1/2+ <i>y</i> , – <i>z</i>
O(19)–H(19)⋯O(17)	0.837(10)	2.128(3)	2.905(5)	154.3(6)	1– <i>x</i> , –1/2+ <i>y</i> , – <i>z</i>
C(7)–H(7a)⋯O(23)	0.950(12)	2.543(6)	3.398(8)	149.8(8)	1– <i>x</i> , –3/2+ <i>y</i> , 1– <i>z</i>
C(30)–H(30)⋯O(1)	1.000(12)	2.245(5)	3.110(7)	144.0(7)	1– <i>x</i> , 1/2+ <i>y</i> , 1– <i>z</i>
C(30)–H(30)⋯O(4)	1.000(12)	2.367(5)	3.232(7)	144.3(7)	1– <i>x</i> , 1/2+ <i>y</i> , 1– <i>z</i>

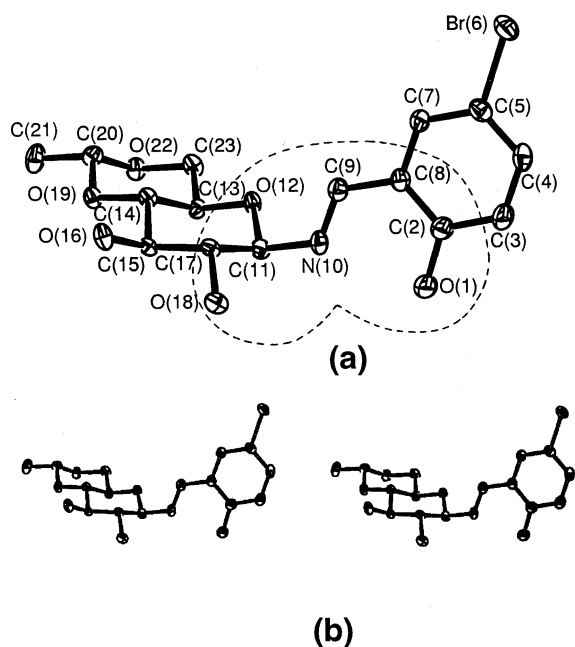


Fig. 4. (a) Molecular structure of **2** and (b) its stereoview showing 50% probability thermal ellipsoids using ORTEP. The dashed line enclosure shown in (a) represents the ONO binding core.

Table 7
Atomic coordinates ($\times 10^4$) for **2**

	x	y	z
C(2)	7325(3)	1699(5)	6230(2)
C(3)	8189(3)	826(8)	5590(2)
C(4)	8228(3)	2032(5)	4857(2)
C(5)	7409(3)	4160(5)	4766(2)
C(7)	6505(3)	5046(5)	5384(2)
C(8)	6453(3)	3826(5)	6125(2)
C(9)	5448(3)	4723(5)	6762(2)
C(11)	4315(3)	4550(5)	8046(2)
C(13)	1715(2)	5961(6)	8193(1)
C(14)	2311(3)	8297(5)	8562(2)
C(15)	3822(3)	7834(4)	9065(2)
C(17)	5027(3)	6689(4)	8516(2)
C(20)	-297(3)	9658(5)	8629(2)
C(21)	-1451(3)	10720(7)	9197(2)
C(23)	116(3)	6373(5)	7757(2)
Br(6)	7491(1)	5876(1)	3774(1)
N(10)	5412(3)	3684(4)	7451(1)
O(1)	7334(2)	464(4)	6935(1)
O(12)	2840(2)	5149(3)	7627(1)
O(16)	4479(2)	9985(3)	9381(1)
O(18)	6327(2)	5823(5)	9012(1)
O(19)	1152(2)	9298(3)	9071(1)
O(22)	-913(2)	7442(3)	8333(1)

g, 2.03 mmol) in EtOH (10 mL). Yield 0.29 g (40%): mp 169–171 °C. UV–Vis [λ_{\max} ; nm (ϵ ;

L cm⁻¹ mol⁻¹]: 261 (21049), 321 (15647), 414 (4843). ¹H NMR (Me₂SO-*d*₆, 300 MHz, ppm): 8.80 (1 H, s, HC=N), 8.62 (1 H, d, *J* 2.9 Hz, ArH), 8.21 (1 H, dd, *J* 2.9, 9.3 Hz, ArH), 7.03 (1 H, d, *J* 9.5 Hz, ArH), 5.68 (1 H, d, *J* 5.5 Hz, SacOH), 5.43 (1 H, d, *J* 5.5 Hz, SacOH), 4.76 (1 H, q, *J* 4.9 Hz, ProtCH), 4.69 (1 H, d, *J* 8.4 Hz, SacH-1), 4.07 (1 H, m, SacH-5), 3.00–3.60 (5 H, m, Sac), 1.25 (3 H, d, *J* 5.1 Hz, ProtCH₃). ¹³C NMR (Me₂SO-*d*₆, 126 MHz, ppm): 167.9, 163.6, 138.5, 128.8, 128.4, 118.6, 117.3, 98.6, 93.6, 79.9, 74.5, 73.0, 67.9, 67.2, 20.2. FABMS *m/z* 355 (M – H⁺, 100%). Anal. Calcd for C₁₅H₂₀N₂O₈: C, 50.56; H, 5.66; N, 7.86; Found C, 50.53; H, 5.14; N, 7.86.

X-ray crystallography.—Standard procedures were used for mounting the crystals. The diffraction data were collected on a Nonius–Kappa CCD machine in the ϕ scan + ω scan mode using Mo K α radiation. Empirical absorption correction was applied on the data. The structures were solved using SHELXS97 and refined using SHELXL97 program packages.¹⁰ The diagrams were generated using ORTEP¹¹ and PLATON99.¹² Full-matrix least-squares refinement on F^2 with anisotropic thermal parameters for all nonhydrogen atoms was used. The hydrogen positions of the –OH groups were picked up from the difference Fourier and were refined with constraints on O–H bond length and temperature factor. All the other hydrogen atoms were geometrically fixed and were treated as riding atoms with fixed thermal parameters. The hydrogen atom data is given under supplementary data. Other details of data collection and structure refinement are provided in Table 1.

3. Results and discussion

4,6-*O*-Ethylidene- β -D-glucopyranosylamine was condensed with substituted salicylaldehydes to give the corresponding Schiff base products as given in Scheme 1. The molecular weights of these products were obtained from the molecular-ion peaks in their respective FAB mass spectra. XRD study of the Schiff base molecules revealed the presence of an interesting ONO tridentate core suitable for

binding. Ours is the first crystallographic characterisation of Schiff bases derived from a glycosylamine.

FTIR studies.—In the FTIR spectra of the glycosylamine-based Schiff base molecules **1**, **2** and **3**, a few strong characteristic bands for saccharides ν_{C-O} were observed in the range 900–1160 cm^{-1} along with the characteristic peaks of aromatic ν_{C-C} in the range 1500–1600 cm^{-1} , revealing the presence of both the saccharide and the aromatic moiety in it; hence, the desired product. These compounds exhibited $\nu_{\text{phenolic OH}}$ in the range 3427–3510 cm^{-1} , and $\nu_{\text{saccharide OH}}$ around 3439, 3397 and 3275 cm^{-1} , for **1**, **2** and **3**, respectively. Products **1**, **2** and **3** showed characteristic peaks for

$\nu_{C=N}$ at 1632, 1627 and 1628 cm^{-1} , respectively, supporting the formation of the imine centre. Fingerprint regions of the spectra were also compared. In the spectrum of the Schiff base derived from 5-nitrosalicylaldehyde, **3**, asymmetric $\nu_{N=O}$ was observed at 1520 cm^{-1} , and the corresponding symmetric stretch was found at 1335 cm^{-1} . Thus, FTIR spectra supported the formation of the desired products.

NMR studies.—NMR Spectra of **1**, **2** and **3** were recorded in $\text{Me}_2\text{SO}-d_6$ and were compared with the spectra of the corresponding saccharide and amine counterparts. Positions of all the exchangeable proton signals were identified by D_2O exchange experiments. In

Table 8
Anisotropic displacement parameters ($\text{\AA}^2 \times 10^3$) for **2**

	U^{11}	U^{22}	U^{33}	U^{23}	U^{13}	U^{12}
C(2)	21(1)	26(2)	28(2)	1(1)	2(1)	4(1)
C(3)	25(1)	30(1)	35(1)	−2(2)	8(1)	9(2)
C(4)	23(1)	31(2)	31(2)	−7(1)	11(1)	2(1)
C(5)	21(1)	31(2)	20(1)	1(1)	4(1)	0(1)
C(7)	21(1)	23(1)	25(1)	−1(1)	4(1)	5(1)
C(8)	16(1)	24(1)	23(1)	−2(1)	3(1)	1(1)
C(9)	20(1)	24(1)	26(2)	−4(1)	3(1)	2(1)
C(11)	15(1)	25(2)	19(1)	1(1)	4(1)	3(1)
C(13)	14(1)	19(1)	20(1)	−1(2)	5(1)	2(2)
C(14)	13(1)	22(1)	18(1)	0(1)	2(1)	−1(1)
C(15)	15(1)	20(1)	13(1)	−1(1)	0(1)	−1(1)
C(17)	12(1)	24(1)	15(1)	2(1)	2(1)	0(1)
C(20)	16(1)	23(1)	25(2)	0(1)	0(1)	3(1)
C(21)	19(1)	35(2)	42(2)	−16(2)	1(1)	6(2)
C(23)	15(1)	31(2)	21(1)	−3(1)	2(1)	−2(1)
Br(6)	37(1)	45(1)	22(1)	4(1)	8(1)	9(1)
N(10)	17(1)	25(1)	23(1)	−5(1)	5(1)	2(1)
O(1)	39(1)	37(2)	32(1)	8(1)	13(1)	18(1)
O(12)	13(1)	28(1)	20(1)	−6(1)	2(1)	2(1)
O(16)	18(1)	28(1)	22(1)	−8(1)	3(1)	−6(1)
O(18)	10(1)	33(1)	22(1)	4(1)	2(1)	0(1)
O(19)	13(1)	28(1)	19(1)	−4(1)	1(1)	3(1)
O(22)	14(1)	27(1)	26(1)	−4(1)	4(1)	−1(1)

The anisotropic displacement factor exponent takes the form: $-2\pi^2[h^2a^{*2}U^{11} + \dots + 2hka \times b \times U^{12}]$.

Table 9
Selected torsion angles ($^\circ$) for **2**

N(10)–C(11)–O(12)–C(13)	178.8(2)	N(10)–C(11)–C(17)–C(15)	172.6(2)
O(12)–C(11)–C(17)–O(18)	170.6(2)	C(14)–C(15)–C(17)–O(18)	−168.8(2)
O(16)–C(15)–C(17)–C(11)	−171.3(2)	C(13)–C(14)–C(15)–O(16)	176.3(2)
O(19)–C(14)–C(15)–C(17)	178.2(2)	O(12)–C(13)–C(14)–O(19)	174.2(2)
C(23)–C(13)–O(12)–C(11)	−174.8(2)	C(23)–C(13)–C(14)–C(15)	174.5(2)
C(8)–C(9)–N(10)–C(11)	−176.0(2)	C(2)–C(8)–C(9)–N(10)	4.5(4)

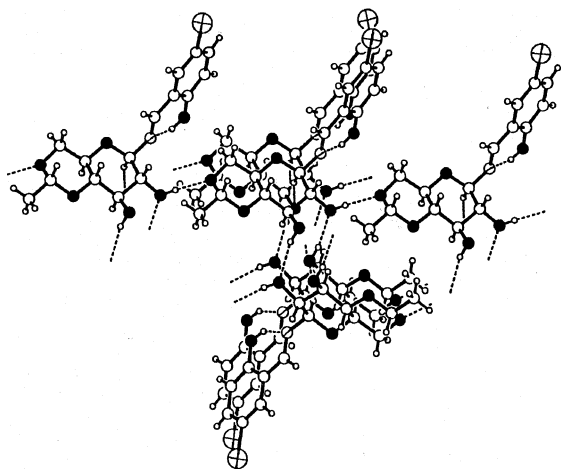


Fig. 5. H-bonding pattern observed in **2**. The filled circles denote oxygen atoms, circles bisected with one line denote nitrogen atoms and circles with cross denote bromine atoms. Dotted lines represent H-bonds.

the case of **1** and **2**, three exchangeable protons corresponding to the phenolic $-OH$, and the C-2 and C-3 OHs of the saccharide moiety were observed, whereas **3** exhibited only two such signals, corresponding to the saccharide $-OH$ groups, but not the phenolic $-OH$. This observation may be attributed to the fact that the phenoxo ion is resonance stabilised in the presence of the nitro group as shown in Scheme 2. The spectra clearly revealed the presence of the saccharide moiety in a single anomeric form in solution. Based on the chemical shifts (4.56–4.69 ppm) and the J values (8.2–8.4 Hz) observed for H-1, the presence of the β anomeric form of the saccharide moiety was identified in all the three products reported in this paper.¹³

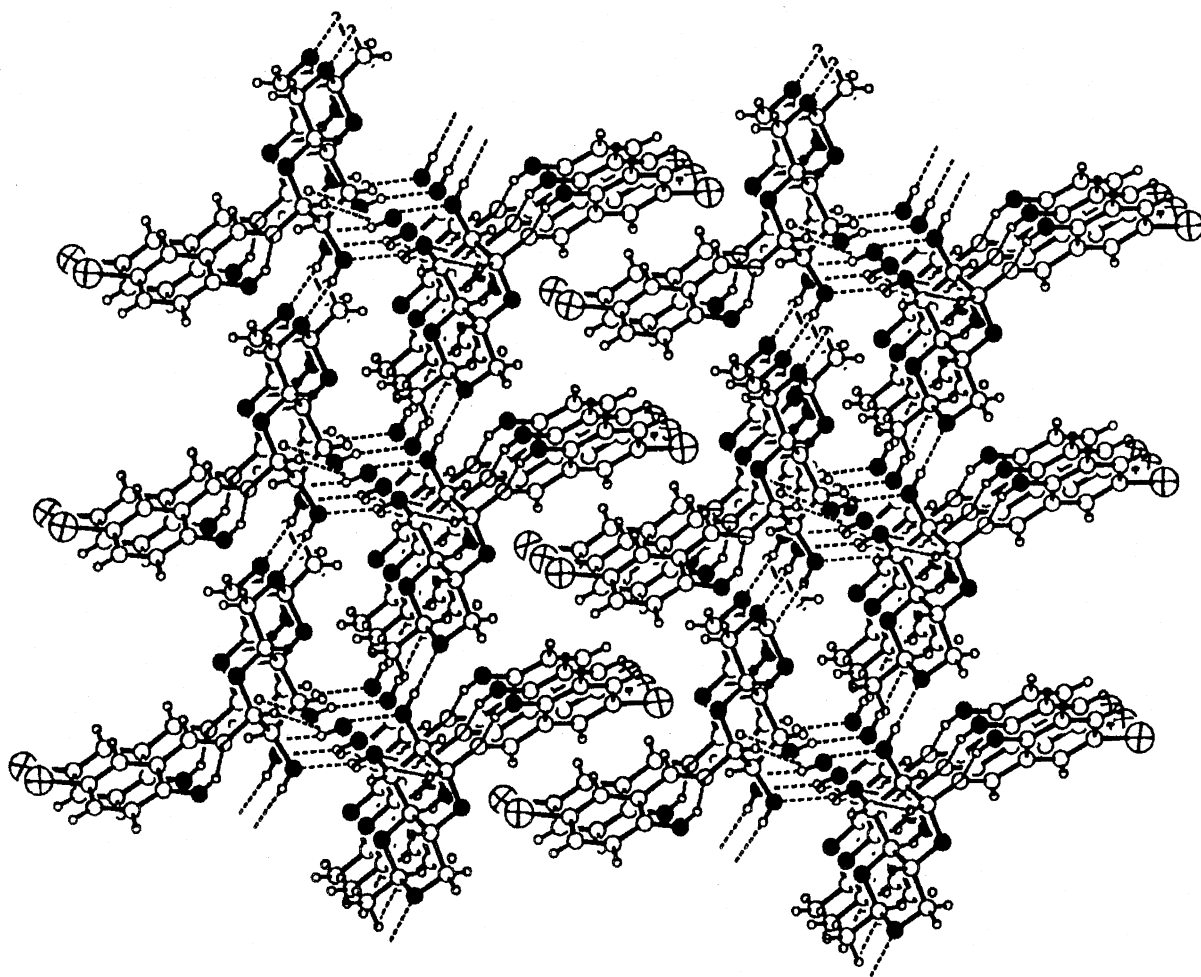


Fig. 6. Packing diagram of **2** showing anti-parallel β -sheet type structure. The filled circles denote oxygen atoms, circles bisected with one line denote nitrogen atoms and circles with cross denote chlorine atoms. Dotted lines represent H-bonds.

Table 10
Hydrogen bond data in the case of **2**

D–H···A	d(D–H) (Å)	d(H···A) (Å)	d(D···A) (Å)	<(DHA) (°)	Symmetry
O(1)–H(1A)···N(10)	0.834 (10)	1.860 (20)	2.588 (3)	145.0 (4)	
O(16)–H(16A)···O(18)	0.836 (10)	1.984 (13)	2.793 (2)	162.6 (3)	1–x, 1/2+y, –z
O(18)–H(18A)···O(22)	0.836 (10)	1.938 (11)	2.771 (3)	174.8 (4)	–1+x, y, z
C(11)–H(11)···O(16)	1.000 (12)	2.403 (23)	3.371 (4)	162.8 (5)	x, –1+y, z

UV–Vis studies.—UV–Vis spectra of all the compounds were measured in Me₂SO using 10^{–2} as well as 10^{–4} M solutions, and the corresponding data is provided in Section 2. Schiff base compounds exhibited three bands in the range 261–420 nm. For both compounds **1** and **2**, very weak bands at 419 nm ($\epsilon = 86 \text{ L cm}^{-1} \text{ mol}^{-1}$) and 414 nm ($\epsilon = 61 \text{ L cm}^{-1} \text{ mol}^{-1}$), respectively, were found. The same band for **3** was found to be very strong at 414 nm ($\epsilon = 4843 \text{ L cm}^{-1} \text{ mol}^{-1}$). This may be attributed to the fact that the –NO₂ group is a chromophore, and in the solution, the phenolic –OH (an auxochrome) is deprotonated due to the presence of the nitro group, which enhances the molar absorptivity. Deprotonation of the phenolic –OH in the Me₂SO solution was also supported by NMR spectra. The red shift observed in the case of the methoxy derivative with respect to its other analogues may be attributed to the presence of the –OMe group, which acts as an auxochrome.¹⁴

Single crystal X-ray studies.—In the case of **1** and **2**, the molecules crystallised in a monoclinic lattice. One chloroform molecule was associated with compound **1**, but no such association with a solvent molecule was observed in the case of **2**.

Molecular structure of 1.—The molecular structure of **1** revealed the pyranose form of the saccharide moiety, with the 4- and 6-positions as being protected by an ethylidene group, and the C-1 being modified through Schiff base formation. An ORTEP view of the molecule is shown in Fig. 1(a). Atomic coordinates and the temperature parameters are given in Tables 2 and 3, respectively. The bond lengths and bond angles in the structure are quite normal and hence this information is given in Section 5. A stereoview of this molecule, Fig. 1(b), supports the presence of

the saccharide in the ⁴C₁ conformation along with its β anomeric form, which was also indicated by the NMR study. The stereoview further reveals the chair conformation of both of the 5-membered rings, resulting from the saccharide moiety and its protection at the 4- and 6-positions. The presence of the β -anomeric form of the saccharide moiety is also understood based on the torsion angles, i.e., N(11)–C(12)–O(13)–C(14) = 179.4°(4) and N(11)–C(12)–C(18)–C(16) = 177.7°(4). Analysis of the torsion angles (Table 4) revealed the trans-orientation of the saccharide moiety and aromatic rings with respect to the C=N bond [C(9)–C(10)–N(11)–C(12) = 178.8°(4)], and the cis-orientation of the phenolic –OH group and imine nitrogens [C(2)–C(9)–C(10)–N(11) = 0.5°(6)]. This structure favours the formation of an interesting ONO tridentate binding core comprised of the phenolic –OH, the imine nitrogen, and the saccharide 2-OH group as shown by an enclosure in Fig. 1(a). Cremer–Pople parameters¹⁵ as well as asymmetry parameters¹⁶ for **1** and **2**, obtained using the program PLATON99, are given in Table 5.

Lattice structure of 1.—The lattice structure of this molecule exhibited a six-atom intramolecular hydrogen bonding interaction between the phenolic –OH and the imine nitrogen. In the lattice, while the 2-OH and 3-OH of the saccharide moiety of each ligand acts as a hydrogen donor towards another molecule, 3-OH and 4-O acts as a hydrogen acceptor towards a third molecule. Thus, in the lattice, each molecule is linked with two other molecules through four intermolecular O–H···O interactions. In addition, the molecule also exhibited three weak C–H···O type interactions, viz., Cl₃C–H···O_{phenolic}, Cl₃C–H···O_{methoxy} and Ar–C–H···O–C-6(sac). All such interactions found around each molecule in the lattice are shown in Fig. 2. In

the lattice, dimers are formed due to the presence of two Ar–C–H \cdots O–C-6 interactions. These dimers are further connected to form chains through two O–H \cdots O interactions of the type, C-2–OH \cdots O–C-3 and C-3–O \cdots HO–C-2. The chains thus formed, stack to result in large size rectangular type cavities with dimensions 12.2 and 6.8 Å, which hold two CHCl₃ molecules using two interactions of the type Cl₃C–H \cdots O_{methoxy} and Cl₃C–H \cdots O_{phenoxy}. These cavities can be observed as channels when the stacking of molecules in the lattice is viewed in the third dimension as shown in Fig. 3. The metric parameters of these interactions are given in Table 6.

Molecular structure of 2.—The molecular structure of **2** is shown in Fig. 4(a). Atomic coordinates and the temperature parameters are given in Tables 7 and 8, respectively. The bond lengths and the bond angles in the structure are quite normal, and hence this information is given in Section 5. Even in this case, the stereoview shown in Fig. 4(b), revealed the saccharide moiety in the ⁴C₁ conformation as the β anomer. The saccharide and the aromatic moieties maintained a trans-orientation with respect to the C=N bond, and this orientation resulted in the formation of an ONO tridentate core that is specially oriented for chelation, as shown by an enclosure in Fig. 4(a). The torsion angles given in Table 9 support these features.

Lattice structure of 2.—In the lattice, this molecule possesses one intramolecular and five intermolecular hydrogen-bonding interactions. Out of five intermolecular interactions, four are of the O–H \cdots O type and one is of the C–H \cdots O type. Like the previous case, even in this one, the intramolecular hydrogen bonding interactions arise due to the close proximity of the phenolic OH and the imine nitrogens. Between the lattice structures of **1** and **2**, major differences lie in the nature of the intermolecular interaction as well as the donor and acceptor centres. In this case, the 2-OH group acts as both the hydrogen donor and the acceptor, whereas the 3-OH group acts only as the hydrogen donor, and the 6-O acts as acceptor instead of the 4-O group. Thus, the 2-OH acts as donor towards the 6-O of a

neighbouring molecule, and the 3-OH acts as donor towards the 2-OH of a different neighbouring molecule. Similarly, the molecule acts as acceptor towards two other molecules in the lattice. Therefore, in this case every molecule is linked with four other molecules through O–H \cdots O interactions and with one other molecule through C-1–H \cdots OH–C-3 type interactions as shown in Fig. 5. Thus, in the lattice, the molecules are interconnected through C-2–OH \cdots O–C-6 to form chains, where the phenyl moieties protrude out of the chain with an inclined angle with respect to the axis of propagation of the chain. Two such adjacent chains or strands are connected together as in an antiparallel β-sheet through hydrogen-bond interaction of the type C-3–OH \cdots O–C-2 and C-2–O \cdots HO–C-3. Packing of such dimeric chains in the lattice results in the stacking of phenyl rings. Stacking of the chains in the third dimension results in the formation of channels, as shown in Fig. 6, having dimensions of 7.4 and 4.6 Å. These channels are smaller than those observed in case of **1**. Metric parameters for weak interactions are listed in Table 10.

4. Conclusions

D-Glucose was successfully modified into the corresponding Schiff base molecules through partial protection and glycosyl amination, followed by condensation with substituted salicylaldehydes. Such modifications facilitate the solubility of the resulting Schiff base products in nonaqueous solvents and lock the saccharide in the β-anomeric form, even in the solution. Such also assists in the formation of single crystals of the products. X-ray diffraction study of the molecules reveals the pyranose form of the saccharide moiety, with the 4- and 6- positions being protected by the ethylidene moiety. The C-1–NH₂ is modified to give a Schiff base, –C-1–N=C(H)–. The same study also reveals the ⁴C₁ chair conformation of the saccharide moiety as the β-anomeric form even in the solid state. A stereoview of the molecules shows the presence of an interesting ONO tridentate chelating core. Metal-ion binding to such an ONO core is expected to result in one six-

membered and another five-membered chelate, and work is currently in progress in our laboratory to investigate the formation of their possible complexes. Recently, we reported the interaction of metal ions with an anthranilic acid based glycosylamine, viz., *N*-(*O*-carboxyphenyl)-4,6-*O*-ethylidene- β -D-glucopyranosylamine.⁷ The crystal lattices of **1** and **2** exhibit a number of O–H \cdots O and C–H \cdots O interactions that result in interesting structures. The lattice of **1** exhibits a channel type structure where the channels are filled with chloroform molecules. Moreover, the lattice **2** exhibits an antiparallel β -sheet type structure where two strands consisting of saccharide molecules are held together by hydrogen-bonding interactions, and the aromatic moieties protrude out of these strands and are stacked.

5. Supplementary material

Full crystallographic details, excluding structure factors, have been deposited with Cambridge Crystallographic Data Centre for structures **1** (CCDC 166682) and **2** (CCDC 166683). These data may be obtained, on request, from The Director, CCDC, 12 Union Road, Cambridge CB2 1EZ, UK (Fax: +44-1223-336033; e-mail: deposit@ccdc.cam.ac.uk or www: <http://www.ccdc.cam.ac.uk>).

Acknowledgements

C.P.R. acknowledges financial support from the Council of Scientific and Industrial Research, Department of Science and Technology and Board of Research in Nuclear

Sciences of Department of Atomic Energy. We thank RSIC, CDRI Lucknow for Mass and RSIC, IIT Bombay for some NMR spectra, and Mr Kuppinen for some experimental help.

References

- Paulsen, H.; Pflughaupt, K.-W. In *The Carbohydrates: Chemistry and Biochemistry*; Pigman, W.; Horton, D., Eds. Glycosylamines, 2nd ed.; Academic: New York, 1980; Vol. 1B, pp. 881–927.
- Lai, H.-Y. L.; Axelrod, B. *Biochem. Biophys. Res. Commun.* **1973**, *54*, 463–468.
- Truscheit, E.; Frommer, W.; Junge, B.; Müller, L.; Schmidt, D. D.; Wingender, W. *Angew. Chem., Int. Ed. Engl.* **1981**, *20*, 744–761.
- Walker, D. E.; Axelrod, B. *Arch. Biochem. Biophys.* **1978**, *187*, 102–107.
- Isbell, H. S.; Frush, H. L. *J. Org. Chem.* **1958**, *23*, 1309–1319.
- Fragoso, A.; Kahn, M. L.; Castiñeiras, A.; Sutter, J.-P.; Kahn, O.; Cao, R. *Chem. Commun. (Cambridge)* **2000**, 1547–1548.
- Sah, A. K.; Rao, C. P.; Saarenketo, P. K.; Wegelius, E. K.; Rissanen, K.; Kolehmainen, E. *J. Chem. Soc., Dalton Trans.* **2000**, 3681–3687.
- Linek, K.; Alfoldi, J.; Durindova, M. *Chem. Pap.* **1993**, *47*, 247–250.
- Brewster, C. M.; Millam, L. H. *J. Am. Chem. Soc.* **1933**, *55*, 763–766.
- Sheldrick, G. M. *shelx97 Programs for Crystal Structure Analysis (Release 97-2)*; Institut für Anorganische Chemie der Universität: Göttingen, Germany, 1998.
- Burnett, M. N.; Johnson, C. K. *ORTEP III, Report ORNL-6895*; Oak Ridge National Laboratory: Oak Ridge, TN, USA, 1996.
- Spek, A. L. *Acta Crystallogr., Sect. A* **1990**, *46*, C34.
- Silverstein, R. M.; Bassler, G. C.; Morrill, T. C. *Spectroscopic Identification of Organic Compounds*, 5th ed.; Wiley: New York, 1991; pp. 221–221.
- Skoog, D. A.; Leary, J. J. *Principles of Instrumental Analysis*, 4th edition; Harcourt Brace College: USA, 1992; pp. 150–173.
- Cremer, D.; Pople, J. A. *J. Am. Chem. Soc.* **1975**, *97*, 1354–1358.
- Duax, W. L.; Weeks, C. M.; Rohrer, D. C. *Top. Stereochem.* **1976**, *9*, 271–383.